Radiotherapy and Oncology 141 (2019) 256–261

Contents lists available at ScienceDirect

Radiotherapy and Oncology

journal homepage: www.thegreenjournal.com

Original Article

Low doses of ionizing radiation activate endothelial cells and induce angiogenesis in peritumoral tissues

Filipa Gil Marques [a], Esmeralda Poli [b,1], João Malaquias [c,1], Tânia Carvalho [d], Ana Portêlo [e], Afonso Ramires [c], Fernando Aldeia [c], Ruy Miguel Ribeiro [f], Emília Vitorino [g], Isabel Diegues [b], Luís Costa [h], João Coutinho [c], Filomena Pina [b], Marc Mareel [i], Susana Constantino Rosa Santos [a,*]

[a] *Angiogenesis Laboratory, Centro Cardiovascular da Universidade de Lisboa, Faculdade de Medicina, Universidade de Lisboa;* [b] *Radiotherapy Service, Centro Hospitalar Universitário Lisboa Norte;* [c] *Department of Surgery, Centro Hospitalar Universitário Lisboa Norte;* [d] *Histology and Comparative Pathology Laboratory, Instituto de Medicina Molecular; Faculdade de Medicina, Universidade de Lisboa;* [e] *Instituto de Medicina Molecular; Faculdade de Medicina, Universidade de Lisboa;* [f] *Biomathematics Laboratory, Faculdade de Medicina, Universidade de Lisboa;* [g] *Department of Pathology, Centro Hospitalar Universitário Lisboa Norte;* [h] *Oncology Department, Centro Hospitalar Universitário Lisboa Norte; Instituto de Medicina Molecular; Faculdade de Medicina, Universidade de Lisboa, Portugal; and* [i] *Department of Radiotherapy and Laboratory of Experimental Cancer Research, Ghent University Hospital, Belgium*

ARTICLE INFO

Article history:
Received 4 February 2019
Received in revised form 24 June 2019
Accepted 27 June 2019
Available online 31 July 2019

Keywords:
Angiogenesis
Ionizing radiation
Radiotherapy
Microvasculature
Endothelial cell activation

ABSTRACT

Purpose: During radiotherapy the peritumoral tissues are daily exposed to subtherapeutic doses of ionizing radiation. Herein, the biological and molecular effects of doses lower than 0.8 Gy per fraction (LDIR), previously described as angiogenesis inducers, were assessed in human peritumoral tissues.
Material and methods: Paired biopsies of preperitoneal adipose tissue were surgically collected from 16 patients diagnosed with locally advanced rectal cancer who underwent neo-adjuvant radiotherapy. One of the biopsies is located in the vicinity of the region where the tumor received the prescribed dose of radiation, and thus exposed to LDIR; the other specimen, outside all beam apertures, was used as an internal calibrator (IC). Microvessel density (MDV) was quantified by immunohistochemistry and the expression of several pro-angiogenic genes was assessed by quantitative RT-PCR using exclusively endothelial cells (ECs) isolated by laser capture microdissection microscopy.
Results: LDIR activated peritumoral ECs by significantly up-regulating the expression of several pro-angiogenic genes such as *VEGFR1*, *VEGFR2*, *ANGPT2*, *TGFB2*, *VWF*, *FGF2*, *HGF* and *PDGFC*. Accordingly, the MVD was significantly increased in peritumoral tissues exposed to LDIR, compared to the IC. The patients that yielded a larger pro-angiogenic response, also showed the highest MVD.
Conclusions: LDIR activate ECs in peritumoral tissues that are associated with increased MVD. Although the technological advances in radiotherapy have contributed to reduce the damage to healthy tissues over the past years, the anatomical regions receiving LDIR should be taken into account in the treatment plan report for patient follow-up and in future studies to correlate these doses with tumor dissemination.

Radiotherapy is widely used to treat malignant tumors. It is mostly delivered in fractionated schemes, consisting of a daily small dose repeated during several weeks until a potentially curative dose has accumulated inside the tumor volume [1]. However, it is important to consider that shaped ionizing radiation beams intersect at the tumor site from successive angles, resulting in significant exposure of nearby healthy tissues to a wide range of daily subtherapeutic doses of ionizing radiation (SDIR). These SDIR can induce different biological effects. High to moderate SDIR are described as promoting human cardiotoxicity and radiation pneumonitis after breast cancer radiotherapy [2–4]. Strikingly, we previously demonstrated that moderate to low doses of SDIR (doses lower or equal to 0.8 Gy, here referred to as LDIR) activate ECs and promote neovascularization in different experimental models [5,6]. *In vitro*, doses lower than 0.8 Gy induce a rapid phosphorylation of several endothelial cell proteins, including VEGF [6] and consequently activate the endothelium and modulate the expression of pro-angiogenic factors [5]. Using different animal models, we showed that LDIR promote angiogenesis during zebrafish development or adult fin regeneration (0.5 Gy) and in a murine Matrigel assay (0.3 Gy) [6]. In a mouse model of hindlimb ischemia, LDIR stimulated neovascularization (0.3 Gy administered during 4 consecutive days) [5]. Interestingly, using murine tumor models

* Corresponding author at: Centro Cardiovascular da Universidade de Lisboa, Faculdade de Medicina, Universidade de Lisboa, Avenida Prof. Egas Moniz, Edificio Egas Moniz, 1649-028 Lisboa.
E-mail address: sconstantino@medicina.ulisboa.pt (S.C. Rosa Santos).
[1] Equal authorship.

https://doi.org/10.1016/j.radonc.2019.06.035
0167-8140/

whole body LDIR (0.3 Gy) promoted tumor growth and metastasis formation by enhancing angiogenesis [6]. Since whole body exposure was applied, the data suggest that LDIR do not change the metastatic organotropism. Considering these observations, we were interested in investigating the effect of LDIR in the vasculature of peri-tumoral tissues, in humans. In the present study, two biopsies of preperitoneal adipose tissue were surgically removed from patients diagnosed with locally advanced rectal cancer who underwent neo-adjuvant radiotherapy treatment: (i) a specimen located in the vicinity of the tumor, and thus exposed to LDIR; and (ii) a specimen outside all beam apertures that was used as an IC for each patient. MVD was quantified and endothelial cell gene expression pattern for several pro-angiogenic genes was assessed.

Materials and methods

Patient material

Samples were collected prospectively from patients diagnosed with locally advanced rectal cancer receiving neoadjuvant radiotherapy followed by curative surgery at Santa Maria Hospital, CHULN (Lisbon, Portugal), between 2013 and 2017. Eligibility criteria included: (i) anatomic pathology diagnosis of rectal adenocarcinoma (Stages II and III); (ii) no radiologic evidence of metastatic disease; (iii) setup of RT treatment in the supine position; (iv) age between 30 and 65 years old; (v) absence of a concomitant malignancy or a non-malignant systemic disease, including diabetes and active infections; and (vi) absence of prior treatment for rectal cancer (surgery, RT or chemotherapy).

The institutional review board provided ethical approval of the study, which complied with all national regulations and the Declaration of Helsinki.

Patients underwent 3D-conformal RT delivering 50.40 Gy in 28 fractions of 1.8 Gy, 5 consecutive days per week, and concurrent leucovorin (20 mg/m^2/day) with 5-fluorouracil (425 mg/m^2/day) administered during the first 4 days in the first week then restarted for 3 days in the fifth week of the treatment course or capecitabine via oral administration (825 mg/m^2 twice a day). All patients received a cumulative tumor dose of 50.40 Gy, between 38 and 48 days. Overall cancer treatment was provided as per the institutional guidelines.

During classic surgical approach, every patient underwent rectal anterior resection, 8 weeks after completion of the neoadjuvant radiotherapy. The procedure was always performed by the same surgeon. Two biopsies of preperitoneal adipose tissue adjacent to the *rectus abdominis* muscle and located deeper than the build-up region of the photon beam were collected from areas corresponding to: (i) tissues exposed to SDIR during neoadjuvant RT (10–40% of the therapeutic dose; referred to as LDIR); and (ii) tissues outside all beam apertures, exposed to doses below 2% of the therapeutic dose (referred to as IC). Before incision, the surgeon precisely identified biopsy sites according to established parameters determined in the treatment planning of each patient, which included one internal body reference (the top of the right iliac crest) and the skin markers established during RT (at supine position). The samples were then precisely resected with an error margin of 1 cm in diameter, not compromising the areas of interest.

After resection, tissue samples were cut into two equal parts: one was immediately placed in a cryomold, embedded in OCT (Optimal Cutting Temperature, Tissue Rek ®) compound, snap-frozen in cold isopentane and liquid nitrogen and then stored at −80 °C to be used for LCM and molecular analysis, while the other sample was formalin-fixed and paraffin embedded to be used for immunohistochemistry.

Laser capture microdissection

Samples stored at −80 °C were cryosectioned in serial sections of 12 μm and mounted on pre-cooled RNAse-free glass microscope slides (Carl Zeiss Microscopy GmbH). The immunohistochemistry for CD31 followed by microdissection of ECs were performed as previously described [5]. For each sample, an area of 1 500 000 μm^2 was collected.

RNA extraction, cDNA synthesis and quantitative real-time PCR

Total RNA was extracted from the microdissected ECs using the RNeasy® Micro Kit (QIAGEN) as described [5]. For synthesis and preamplification of cDNA, RT^2 Nano PreAMP cDNA synthesis Kit (SABiosciences, QIAGEN) was used with three rounds of preamplification using the following human genes: *VEGFR1*; *VEGFR2*; *ANGPT2*; *TGFB2*; *VWF*; *FGF2*; *PDGFC*; *HGF*; *PLG*; *COL18A1*; *HIF1AN*; *HIF1A*; *END1*; *FBLN1*; *SPOCK1*; *COL4A1*; *COL4A2* and *r18S*. The sequences of the primers are detailed in Supplementary materials and the mRNA expression was assessed as described [5].

Immunohistochemistry

Preperitoneal adipose tissue samples were fixed in 10% neutral-buffered formalin, embedded in paraffin and 5-μm sections were mounted on glass slides. Endogenous peroxidase activity was blocked with 0.3% hydrogen peroxide (H_2O_2) in methanol, for 30 min, followed by 3 washes in PBS, for 30 min. Sections were incubated for 1 hour, with a mouse monoclonal antibody against the human von Willebrand Factor (vWF; clone M0616; DAKO) at 1:200, diluted in PBS-1% BSA. After 3 washes in PBS, for 30 min, a secondary biotinylated goat anti-mouse antibody (Vector Laboratories) was added, at 1:200, in PBS, for 30 min. Washes were performed as before and the labeling and counterstaining procedures followed as described [5]. MVD was evaluated by counting the number of vWF-positive microvessels in slides digitally scanned in NanoZoomer SQ (Hamamatsu Photonics K. K.) running NDP.view2 software. MVD, i.e. number of microvessels per adipocyte per high power field, was measured by two independent observers including a pathologist blinded to experimental groups in at least three hot-spots at 20x original magnification, using ImageJ® software. Due to technical limitations found in at least one of the two biopsies, it was not possible to determine the MVD in 6 out of the 16 patients (P5, P6, P10, P12, P14 and P16).

Statistical analysis

Figure's data are shown as mean ± SEM and analyzed with SPSS 20.0 software. Normality was determined for all numeric data by the Shapiro–Wilk test. Two-sided Student's *t*-test for paired samples was used to identify differences between experimental conditions regarding *vWF* and MVD, as these data followed a normal distribution. The Wilcoxon matched-pairs test for related samples was used to assess the endothelial gene expression as normality could not be assumed. *p-values* lower than 0.05 were considered statistically significant. To discriminate endothelial gene expression profile considering each patient's contribution to the global response, a principal component analysis (PCA) was performed using R factoextra and FactoMineR packages [7,8].

Results

The scheme in Fig. 1A summarizes the main steps followed by the patients from the moment that they were included in the study to the moment the biopsies were collected. After their inclusion at the moment of the RT appointment, the CT simulation and the RT

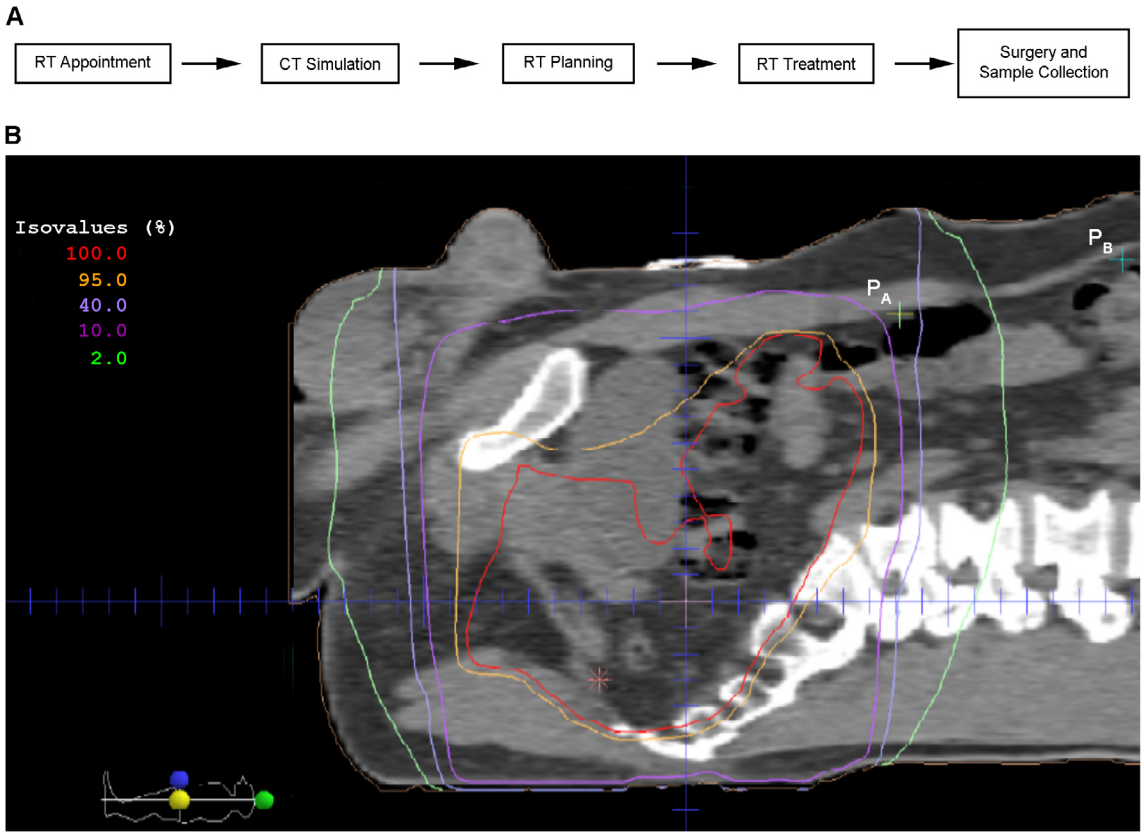

Fig. 1. (A) Schematic representation of the methodological approach used in this study. (B) Sagittal view from computed tomography (CT) images of the radiotherapy (RT) planning in locally advanced rectal cancer. (P_A) and (P_B) represent the locations of the interest and control points, respectively. Point A (P_A) is located between the isodose curves purple and light blue, which represent the isodose areas of 10% and 40% of the prescribed dose, respectively. Point B (P_B) represents the IC biopsy, where the dose is lower than 2% of the prescription. The light green line represents the 2% isodose curve. The red isodose curve (100%) represents the line where the dose is normalized to the prescribed dose of 50.40 Gy. The area inside the orange curve represents the therapeutic area.

planning were performed, before radiotherapy. Eight weeks after the end of the radiotherapy treatment, the surgery was performed and two distinct biopsies, whose locations are defined during the RT planning, were collected from each patient. For each patient's plan, the isodose curves are established and the area of 10% and 40% of the prescribed dose identified. This particular area corresponds to the area of interest in our study and comprises the tissues exposed to daily doses ranging from 0.18 to 0.72 Gy (LDIR). These doses have been already described as being able to activate ECs *in vitro* and of enhancing neovascularization in experimental *in vivo* models [5,6]. In a representative sagittal view from a CT image of the radiotherapy planning (Fig. 1B), the area of interest is represented between the purple and light blue isodose curves and the biopsy site is defined as P_A, a reference point that is inside the area of interest. Simultaneously, in each plan, a second area of interest that will correspond to the IC tissues is determined and defined as P_B, a control point that is as far as possible of the 2% isodose curve, defined by the light green line. Both, P_A and P_B, were excised during surgery taking into account the internal and external anatomical references established during radiotherapy planning.

Patients included in the study were between 38 and 65 years old, and most of them were males (69%). According to the Anatomical Pathology reports, about 81% of all patients were diagnosed with stage III-B rectal cancer (TNM staging system) and 88% of the tumors corresponded to grade I-II. All patients underwent neo-adjuvant radiotherapy with a total prescribed dose of 50.40 Gy (Table 1).

Table 1
Patient characteristics.

	Total
Age (years)	
Media ± SD	51 ± 8.0
[Range]	38–65
Sex (%)	
Female	5 (31%)
Male	11 (69%)
Histological Type (%)	
Adenocarcinoma	16 (100%)
Histologic Grade (G) (%)	
G1-Well differentiated	7 (44%)
G2-Moderately differentiated	7 (44%)
GX-Unknown	2 (12%)
TNM Staging (%)	
Stage II-A	1 (6%)
Stage III-A	2 (13%)
Stage III-B	13 (81%)

To investigate whether LDIR could activate peritumoral ECs, the paired biopsies collected from each patient were stained for CD31, ECs were isolated using a laser capture microdissection microscope (LCM) and gene expression was assessed by quantitative RT-PCR for the following targets: *VEGFR1*, *VEGFR2*, *ANGPT2, TGFB2, VWF, FGF2, HGF* and *PDGFC* (Fig. 2). Transcripts for all of these genes were significantly up-regulated in ECs isolated from peritumoral tissues exposed to LDIR, when comparing to IC tissues (Fig. 2A).

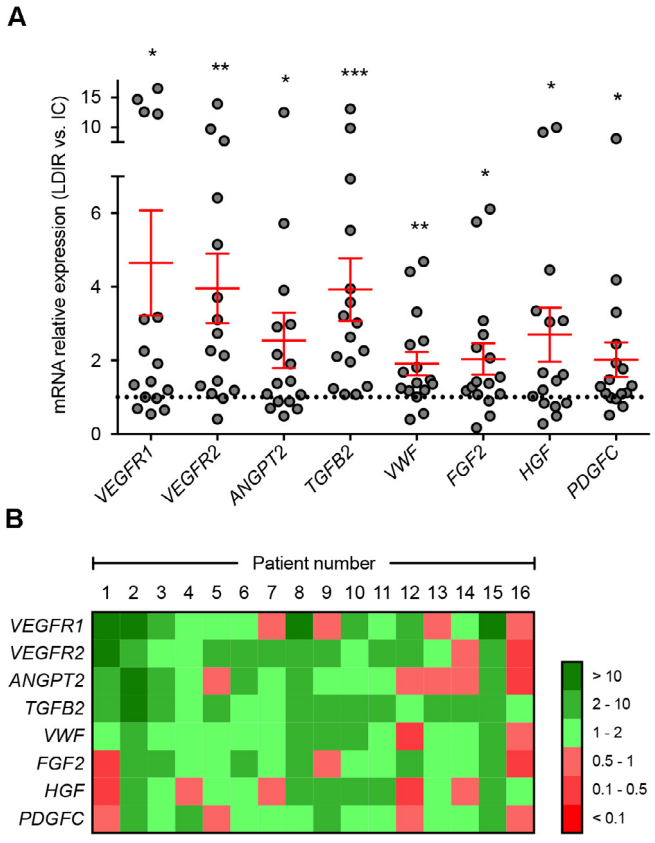

Fig. 2. LDIR are associated with a pro-angiogenic signature in peritumoral ECs. Biopsy sections were immunostained for CD31, followed by ECs isolation by LCM and qRT-PCR. (A). Individual data and mean ± SEM (in red) are shown (n = 16 patients). Data represent the fold change in gene expression relative to the IC (dashed line). Values were normalized to 18S to obtain relative expression levels. Paired two-tailed *t*-test was used to evaluate the differences in VWF gene expression levels, while the Wilcoxon matched-pairs test for related samples was used to assess endothelial gene expression levels as normality could not be assumed. $^{*}P < 0.05$; $^{**}P < 0.01$; $^{***}P < 0.001$. IC: Internal Calibrator. (B) Colored map illustrating differential gene expression levels for each pro-angiogenic target among the population. Green and red colors represent high and low relative gene expression, respectively.

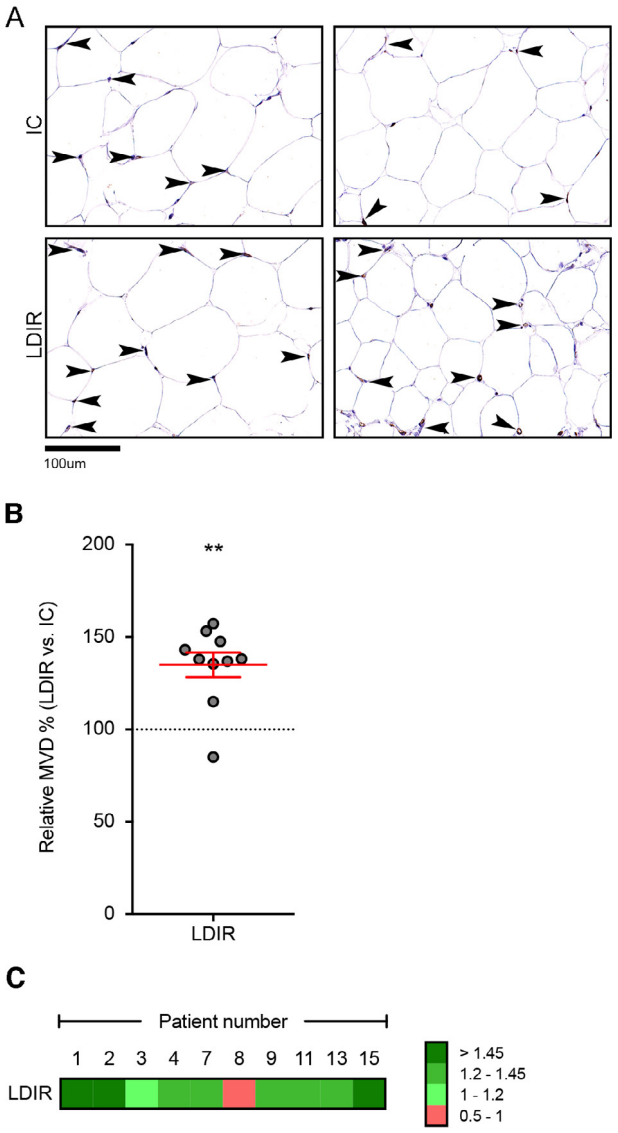

Fig. 3. LDIR are associated with an increase in the MVD of peritumoral tissues. (A) Representative microphotographs of patient tissues exposed to LDIR (lower panel) or IC tissues (upper panel). The tissue is mainly composed of adipose tissue, associated to numerous small capillaries (black arrowhead), here immunostained with anti-vWF antibody (B) Quantitative analysis of the MVD (number of capillaries/adipocyte/field) is shown as percentage relative to the IC (dashed line) for each patient (percentage of a pairwise normalization). Individual data and mean ± SEM (in red) are shown (n = 10 patients). Values assumed normal distribution, equal variance and paired two-tailed *t*-test was used. $^{**}P < 0.01$. IC: Internal Calibrator. (C) Colored map illustrating the differential MVD levels for the patient sample. Green and red colors represent high and low relative gene expression, respectively.

Next, the MVD was assessed in the same samples (in 10 out of the 16 patients) and we found that the number of vWF-positive microvessels significantly increased in the biopsies exposed to LDIR (Fig. 3B).

Surprisingly, two of the patients (P8 and P3) showed a decrease or only a modest increase in MVD in the peritumoral tissues exposed to LDIR, respectively (Fig. 3C), which are not related with the angiogenic molecular signature found in their ECs (Fig. 2B).

Angiogenesis is regulated by a dynamic balance between pro- and anti-angiogenic genes., Thus, the same cDNA used before was analyzed by quantitative RT-PCR to assess the expression of several anti-angiogenic genes such as *PLG*, *COL18A1*, *HIF1AN*, *HIF1A*, *END1*, *FBLN1*, *SPOCK1*, *COL4A1* and *COL4A2*, even though their expression was neither significant in a global gene expression analysis previously published by us [5], nor modulated by LDIR (data not shown). The two-dimensional results of the principal component analysis (PCA) highlight that (i) the pro-angiogenic gene expression profile (in yellow) is separated distinctly from the anti-angiogenic one (in blue); (ii) the pro-angiogenic genes *VEGFR2*, *TGFB2*, *ANGPT2*, *PDGFC* and *VEGFR1* are more correlated among themselves than with *VWF* or *FGF2*; iii) the anti-angiogenic genes *PLG*, *COL18A1*, *HIF1AN*, *HIF1A*, *FBLN1*, *SPOCK1*, *COL4A1* are more correlated among themselves than with *COL4A2* or *END1* (Fig. 4). Note that the yellow and blue shapes in Fig. 4 were manually added to highlight the separation between the groups of pro- and anti-angiogenic genes, respectively.

Through this analysis, we show three groups of patients: the majority of the patients that present an up-regulation only for the pro-angiogenic genes in response to LDIR (cloud of points in the upper left quadrant of Fig. 4); P8, P3 and P10 expressing high levels of anti-angiogenic genes in response to LDIR; P1, P2 and P15 that in response to LDIR express the highest levels of pro-angiogenic genes.

Even though LDIR do not significantly modulate the expression of anti-angiogenic factors in our population, the fact that patients

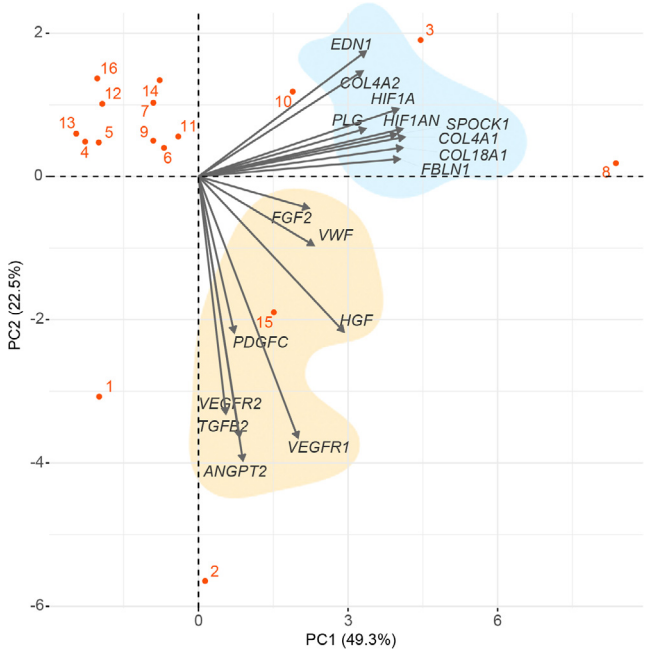

Fig. 4. Two-dimensional principal component analysis (PCA) shows a separation between pro- (in green) and anti-angiogenic (in red) gene expression profiles based on the LDIR stimulus. PC1 explains the variance of anti-angiogenic levels of gene expression, whereas PC2 explains the variance of the pro-angiogenic levels of gene expression. Yellow and blue shapes are not elements of output analysis but only to distinguish pro and anti-angiogenic genes, respectively. The loading axes (for the genes) are not represented for simplicity. The numbered dots represent each patient contribution for the analysis (P1–P16).

P8, P3 and P10 present the highest expression levels of these factors (Fig. 4) could be related with the fact that patients P8 and P3 exhibit the lowest MVD levels (Fig. 3C), since angiogenesis is a balance between pro- and anti-angiogenic factors. Unfortunately, due to technical problems, it was not possible to determine the MVD in patient P10. We also found an interesting relationship in which patients P1, P2 and P15 present the highest expression levels of pro-angiogenic factors (Fig. 4), which are related with their high MVD levels (Fig. 3C).

Discussion

The results of this study are particularly relevant in radiation oncology since they provide insights into the biological effects of LDIR in peritumoral tissues of oncologic patients exposed to radiotherapy and are in line with previous data obtained in experimental models. We have shown that doses lower than 0.8 Gy, referred to as LDIR, activate ECs and promote tumor growth and metastasis in animal models [6]. Acquisition of knowledge about the effect of LDIR on human tissues is challenging since the majority of cancer patients are operated before radiotherapy, termed adjuvant, hampering access to the peri-tumoral tissues of interest. Herein, we conducted a prospective study, selecting rectal adenocarcinoma patients, who underwent neo-adjuvant radiotherapy. For each one of the 16 patients, a radiotherapy planning was performed before radiation treatment allowing for the precise identification of two important areas: one comprises the peritumoral tissues daily exposed to dose ranges of 0.18–0.72 Gy (LDIR); the other corresponds to the IC tissues. Two anatomical references for the biopsies were established for both areas, allowing their precise location and resection during surgery.

The present study provides the first evidence that in human peritumoral tissues, LDIR significantly up-regulate the simultaneous expression of several pro-angiogenic genes. This effect is evident 8 weeks after radiotherapy, suggesting that LDIR tilt the angiogenic balance toward a more pro-angiogenic phenotype for a relatively long period of time. Moreover, this molecular signature appears to have an important impact on function being accompanied by a significant increase in MVD. Interestingly, three of the patients that contributed more to the pro-angiogenic response (P1, P2 and P15), are those that also show higher MVD. In a global gene expression analysis performed in ECs exposed to LDIR, the anti-angiogenic factors were not modulated by LDIR [5]. Accordingly, herein the expression of several anti-angiogenic factors, were not modulated in ECs isolated from peritumoral tissues exposed to LDIR, when compared to cells from the IC tissues. However, it is interesting to note that two of the patients (P8 and P3) that present the highest levels of the anti-angiogenic factors in response to LDIR are those that exhibit the lowest MVD levels. The fact that 3 patients show an up-regulation of anti-angiogenic genes in response to LDIR remains unknown and is certainly due to an additional factor that could be present in these patients and act synergistically with LDIR. Angiogenesis is tightly regulated in physiological setting, in the adult. In these conditions the balance between factors that either stimulate or inhibit the growth of blood vessels is tipped in favor of inhibition and consequently capillary growth is restrained. We found that LDIR up-regulate the expression of pro-angiogenic factors in human peritumoral tissues, concomitant with an increase in the number of microvessels. Importantly, it was shown that the same range of doses of ionizing radiation promotes neovascularization in a hindlimb ischemia model by increasing the capillary and collateral densities [5], disclosing the possibility of using LDIR as a non-invasive and effective tool in the setting of peripheral arterial disease. Interestingly, in that work LDIR induced a sustained and prolonged pro-angiogenic response in ECs still evident 45 days after irradiation [5], suggesting a link for the long-term advantage in blood perfusion, capillary density, and collateral vessel formation.

Technological advances in radiotherapy over the past few decades have contributed to a better local tumor control and reduced tissue damage to normal tissues. Multiple strategies have been developed to target tumoral ECs as a measure to enhance radiotherapy efficacy [9]. Different studies recognize that anti-angiogenic or vascular-destructive agents potentially enhance tumor responses to radiotherapy [10]. Several anti-angiogenics have been clinically evaluated in combination with radiotherapy [11,12]; however, their putative benefits are controversial.

Several signaling pathways and molecules such as ceramide, sphingomyelinase, and Bax were described as regulating EC apoptosis after irradiation with high doses [13–15]. However, it is important to take into consideration that different SDIR will have different biological effects on the vasculature.

In conclusion, this work shows that doses lower than 0.8 Gy per fraction are activators of ECs in human peritumoral tissues and consequently promote increased vascular density. This effect should be taken into account in the treatment plan report for patient follow-up and in future studies to correlate these doses with tumor dissemination. Further research is also warranted to unravel the effects of these LDIR on pre-metastatic niches and their colonization by tumor cells.

Acknowledgments

We thank the Radiotherapy Service, CHULN, Lisbon, Portugal, particularly to C. Raimundo, A. Borges, C. Marques, C. Moreira, D. Parreira, H. Silva, I. Lima, I. Caetano, J. Crespo, L. Rodrigues, M. Rocha, M. Ferreira, M. Pereira, P. Ribeiro, R. Fonseca, R. Branco, S. Lemos, S. Brito, S. Moura, S. Aresta, T. Mouro, T. Leal, and

V. Quintino for help in irradiation delivery. We thank A. Duarte for help in the treatment planning. We thank I. Monteiro Grillo and M. Jorge in the quality of ex-directors of the radiotherapy service and H. Bicha Castelo and J.C. Mendes de Almeida in the quality of ex-directors of the department of surgery for opening the doors when this work started and for their unconditional support. We acknowledge master's students, C. Cardina, J. Ferreira and T. Freitas for their collaboration in this study. We gratefully acknowledge W. de Neve for critically reviewing the manuscript.

Funding

FGM is supported by a PhD fellowship from Universidade de Lisboa, Portugal.

Declaration of Competing Interest

None.

Appendix A. Supplementary data

Supplementary data to this article can be found online at https://doi.org/10.1016/j.radonc.2019.06.035.

References

[1] Moran JM, Elshaikh MA, Lawrence TS. Radiotherapy: what can be achieved by technical improvements in dose delivery? Lancet Oncol 2005;6:51–8. https://doi.org/10.1016/S1470-2045(04)01713-9. PubMed PMID: 15629276.

[2] Curigliano G, Cardinale D, Dent S, Criscitiello C, Aseyev O, Lenihan D, et al. Cardiotoxicity of anticancer treatments: epidemiology, detection, and management. CA Cancer J Clin 2016;66:309–25. https://doi.org/10.3322/caac.21341. PubMed PMID: 26919165.

[3] Oie Y, Saito Y, Kato M, Ito F, Hattori H, Toyama H, et al. Relationship between radiation pneumonitis and organizing pneumonia after radiotherapy for breast cancer. Radiat Oncol 2013;8:56. https://doi.org/10.1186/1748-717X-8-56. PubMed PMID: 23497657; PubMed Central PMCID: PMC3605133.

[4] Taylor C, Correa C, Duane FK, Aznar MC, Anderson SJ, Bergh J, et al. Estimating the risks of breast cancer radiotherapy: evidence from modern radiation doses to the lungs and heart and from previous randomized trials. J Clin Oncol 2017;35(15):1641–9. https://doi.org/10.1200/JCO.2016.72.0722. PubMed PMID: 28319436; PubMed Central PMCID: PMC5548226.

[5] Ministro A, de Oliveira P, Nunes RJ, Dos Santos Rocha A, Correia A, Carvalho T, et al. Low-dose ionizing radiation induces therapeutic neovascularization in a pre-clinical model of hindlimb ischemia. Cardiovasc Res 2017;113:783–94. https://doi.org/10.1093/cvr/cvx065. PubMed PMID: 28444128.

[6] Sofia Vala I, Martins LR, Imaizumi N, Nunes RJ, Rino J, Kuonen F, et al. Low doses of ionizing radiation promote tumor growth and metastasis by enhancing angiogenesis. PLoS ONE 2010;5:. https://doi.org/10.1371/journal.pone.0011222. PubMed PMID: 20574535; PubMed Central PMCID: PMC2888592e11222.

[7] Kassambara AM, Fabien. factoextra: Extract and Visualize the Results of Multivariate Data Analyses. R package version 1.0.5 ed201p. https://CRAN.R-project.org/package=factoextra.

[8] Le S, Josse J, Husson F. FactoMineR: an R package for multivariate analysis. J Stat Softw 2008;25:1–18. PubMed PMID: ISI:000254619400001.

[9] Barker HE, Paget JT, Khan AA, Harrington KJ. The tumour microenvironment after radiotherapy: mechanisms of resistance and recurrence. Nat Rev Cancer 2015;15:409–25. https://doi.org/10.1038/nrc3958. PubMed PMID: 26105538; PubMed Central PMCID: PMC4896389.

[10] Wong P, Houghton P, Kirsch DG, Finkelstein SE, Monjazeb AM, Xu-Welliver M, et al. Combining targeted agents with modern radiotherapy in soft tissue sarcomas. J Natl Cancer Inst 2014;106. https://doi.org/10.1093/jnci/dju329. PubMed PMID: 25326640; PubMed Central PMCID: PMC4207861.

[11] Seiwert TY, Salama JK, Vokes EE. The concurrent chemoradiation paradigm–general principles. Nat Clin Pract Oncol 2007;4:86–100. https://doi.org/10.1038/ncponc0714. PubMed PMID: 17259930.

[12] Shojaei F. Anti-angiogenesis therapy in cancer: current challenges and future perspectives. Cancer Lett 2012;320:130–7. https://doi.org/10.1016/j.canlet.2012.03.008. PubMed PMID: 22425960.

[13] De Meerleer G, Khoo V, Escudier B, Joniau S, Bossi A, Ost P, et al. Radiotherapy for renal-cell carcinoma. Lancet Oncol 2014;15:e170–7. https://doi.org/10.1016/S1470-2045(13)70569-2. PubMed PMID: 24694640.

[14] Fuks Z, Kolesnick R. Engaging the vascular component of the tumor response. Cancer Cell 2005;8:89–91. https://doi.org/10.1016/j.ccr.2005.07.014. PubMed PMID: 16098459.

[15] Garcia-Barros M, Paris F, Cordon-Cardo C, Lyden D, Rafii S, Haimovitz-Friedman A, et al. Tumor response to radiotherapy regulated by endothelial cell apoptosis. Science 2003;300:1155–9. https://doi.org/10.1126/science.1082504. PubMed PMID: 12750523.